View Article Online
View Journal

Green Chemistry

Cutting-edge research for a greener sustainable future

Accepted Manuscript

This article can be cited before page numbers have been issued, to do this please use: L. Gonnet, C. B. Lennox, T. H. Borchers, M. Askari, A. Wahrhaftig-Lewis, S. G. Koenig, K. Nagapudi and T. Friši*ć*, *Green Chem.*, 2026, DOI: 10.1039/D6GC00784H.

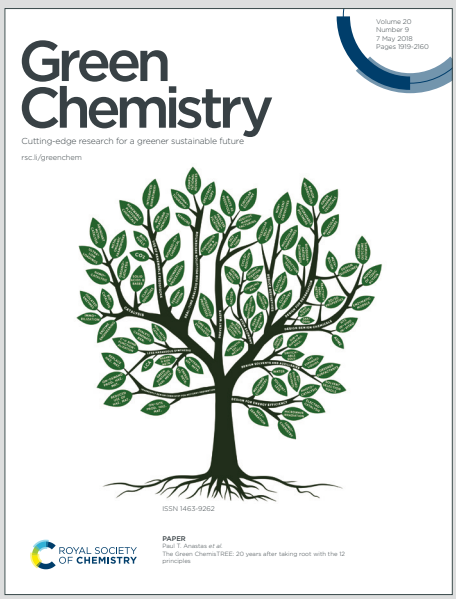

View Article Online
DOI: 10.1039/D6GC00784H

GREEN FOUNDATION BOX

1. This work advances green chemistry by establishing key parameters to design and control reactions using Resonant Acoustic Mixing (RAM) - an emergent, scalable alternative to conventional milling mechanochemistry.

2. This work establishes reactor filling ratio as an important parameter to design RAM-based reactions without bulk solvents, and presents a benchtop methodology for simultaneous real-time following of reaction kinetics, structure of bulk phases, and temperature. Using Buchwald–Hartwig amination as a model, the value of real-time monitoring is evidenced by revealing short-lived temperature increases, means of controlling them, and their role for achieving rapid, high-yielding, multi-gram transformations.

3. This work is a stepping stone towards the rational design of green, RAM-based reactions and could further by enhanced by a deeper understanding of thermal behavior and how it could be effectively controlled for scale-up, reducing catalyst amount, and promoting reactivity of more challenging substrates.

View Article Online
DOI: 10.1039/D6GC00784H

ARTICLE

Establishing Parameters for Resonant Acoustic Mixing (RAM) Chemistry using Buchwald-Hartwig Amination as a Model

Lori Gonnet,[a] Cameron B. Lennox,[a,b] Tristan H. Borchers,[a] Mohammad S. Askari,[a] Alexander Wahrhaftig-Lewis,[a] Stefan G. Koenig*[,c] Karthik Nagapudi*[,c] and Tomislav Friščić*[,a]

`*Received 00th January 20xx, Accepted 00th January 20xx

DOI: 10.1039/x0xx00000x

While Resonant Acoustic Mixing (RAM) has been proposed as a scalable methodology for environmentally-friendly synthesis, notably media-free mechanochemical synthesis, the underlying reaction environment and the parameters that govern reaction control, optimization, and scale-up remain poorly understood. Using the Buchwald-Hartwig amination as a model system, this study provides insight into the RAM reaction environment and establishes design parameters through a combination of systematic screening and multimodal, real-time *in situ* monitoring of reaction progress, temperature evolution, and the transformations of crystalline and non-crystalline bulk phases. The simultaneous application of benchtop infrared thermography, and fingerprint- and terahertz-region Raman (THz-Raman) spectroscopy enables the direct correlation of reactivity, thermal behaviour, and phase evolution. Specifically, this work identifies the filling ratio (φ), acceleration, and the amount of liquid additive (η) as critical parameters to design tunable and scalable (at least 100 mmol) reactivity under RAM conditions, in short timeframes. Real-time monitoring reveals that rapid Buchwald-Hartwig reactivity is associated with autogenous heating, and that φ and acceleration serve as parameters that can be used to control reaction kinetics and temperature evolution. By identifying experimentally accessible reaction control parameters and presenting a benchtop-only design for the simultaneous monitoring of temperature, reaction progress and evolution of transient bulk phases, this work provides a foundation for the rational design, control, and safety of chemistry under RAM conditions.

Introduction

Resonant Acoustic Mixing (RAM)[1] is a highly efficient mixing technology that has recently been used as a scalable technique for chemical[2-6] and material[7-12] synthesis, as well as for high-throughput reaction and cocrystal screening.[13-15] The efficiency and speed of mixing of materials with different rheology has introduced RAM as a highly effective approach for making blends, composites, and materials processing.[16-19] Recently, it has also been used to conduct chemical transformations in the absence of bulk solvent, under solventless or liquid-assisted conditions otherwise only accessible with mechanochemical technologies such as grinding or ball-milling.[10-15] RAM delivers mechanical energy through high-intensity, low-frequency acoustic oscillation of the entire system, and is seen as a "ball-free" alternative to conventional mechanochemical technologies[20] that rely on continuously moving balls, rods, or screws to impart mechanical energy.[21-23] By eliminating these mechanical elements, also known as milling media, RAM significantly simplifies reaction design, facilitates scale-up, and avoids contamination arising as a result of leaching and abrasion from the grinding media. Whereas the potential for high-throughput screening, as well as simplicity of reaction scale-up have been demonstrated in the contexts of material chemistry and catalysis, the parameters which can be used to control and optimize RAM-based reactivity remain poorly understood.

Using as a model the palladium-catalysed Buchwald-Hartwig amination (Fig. 1), arguably one of the key transformations in pharmaceutical and medicinal chemistry[24,25] which is also known to provide safety-related challenges,[26] we now provide a detailed investigation of parameters that can be used to control and optimize RAM-based reactions. This is achieved through extensive screening, real-time *in situ* infrared temperature monitoring (thermography),[27,28] as well as fingerprint Raman, and low-frequency (terahertz, THz) Raman spectroscopy, which enabled an entirely benchtop-based approach to simultaneously gain insight into temperature evolution, reaction kinetics and transformations of bulk crystalline and non-crystalline phases, which would normally require the use of synchrotron X-ray diffraction.[28] Whereas recent work has demonstrated the ability to optimize RAM reactivity through the presence and the amount of liquid additives, as well as by varying the acceleration of the reaction vessels (expressed in the acceleration of gravity, g = 9.81 m·s^{-2}),[4-9] it is now shown that the degree of reactor loading, expressed as the filling ratio (φ, the ratio of the reaction mixture volume to the volume of

[a] School of Chemistry, University of Birmingham, Edgbaston, Birmingham, B15 2TT, UK. E-mail: t.friscic@bham.ac.uk
[b] Department of Chemistry, McGill University, 801 Sherbrooke St. W., H3A 0B8, Montreal, Canada.
[c] Synthetic Molecule Pharmaceutical Sciences, Genentech Inc., One DNA Way, South San Francisco, CA 94080, USA. E-mail: koenig.stefan@gene.com, nagapudi.karthik@gene.com

Supplementary Information available: [details of any supplementary information available should be included here]. See DOI: 10.1039/x0xx00000x

the reaction vessel), can play a critical role in controlling reactivity under RAM conditions. Notably, while recent reports explored how the filling ratio can affect the blending efficiency in RAM, the relationship of φ to chemical reactivity under RAM conditions remains almost completely unexplored.[29,30] Here, the Buchwald-Hartwig amination was chosen as a suitable model for such studies, as it was previously investigated using mechanochemical ball-milling,[31-35] thermochemical,[36-39] or combined thermo-mechanical[40] approaches. We show how varying φ, acceleration, and addition of a liquid additive (expressed as η,[41,42] the ratio of the volume of the liquid additive to the total mass of the reaction mixture, in µL/mg) can be used to affect reaction kinetics and associated thermal behaviour, which is of importance in context of reaction design and safety (Fig. 1). Whereas Buchwald-Hartwig coupling under solventless and ball-milling conditions was previously promoted by external heating,[43] our results show that in RAM such reactivity can be promoted by autogenous heating, without any external heat sources, when operating at high values of φ and acceleration. This leads to rapid (typically within 10-15 minutes), high-yielding, multigram-scale transformations of solid and liquid reactants, with a model reaction scaled to at least 100 mmol, as well as ability to obtain triarylamines, in high conversion compared to corresponding diarylamines, starting from simple aniline precursors. Together with more conventionally used parameters, such as reaction time and catalyst amount, the herein explored variables φ, η, and acceleration provide a broad, versatile set of reaction control parameters under RAM conditions.

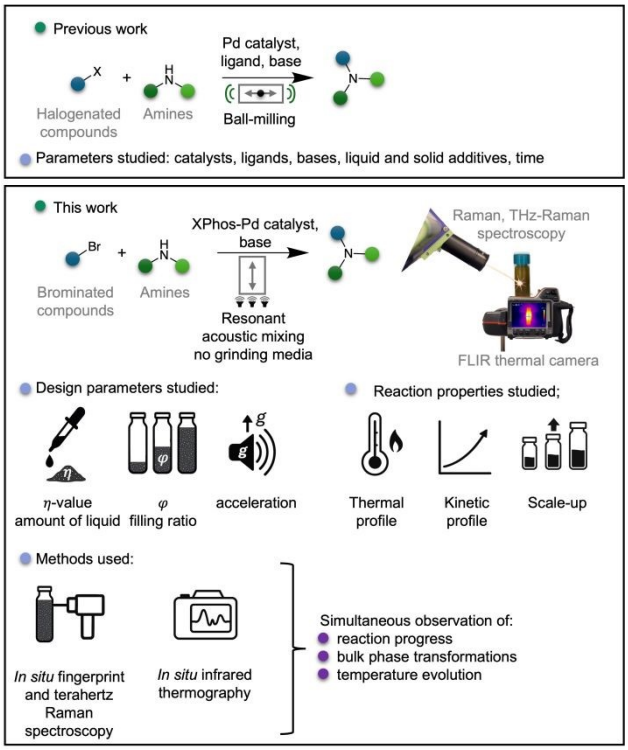

Fig. 1. Comparison of the methods and parameters addressed in previous studies[31-35] of mechanochemical Buchwald-Hartwig reactivity by ball-milling, and in the present investigation of RAM-based reactivity.

Results and discussion

As a benchmark reaction, we focused on the Buchwald-Hartwig coupling of two solid reactants, 1-bromopyrene and diphenylamine, to give **1a** (Fig. 2a), which was previously also

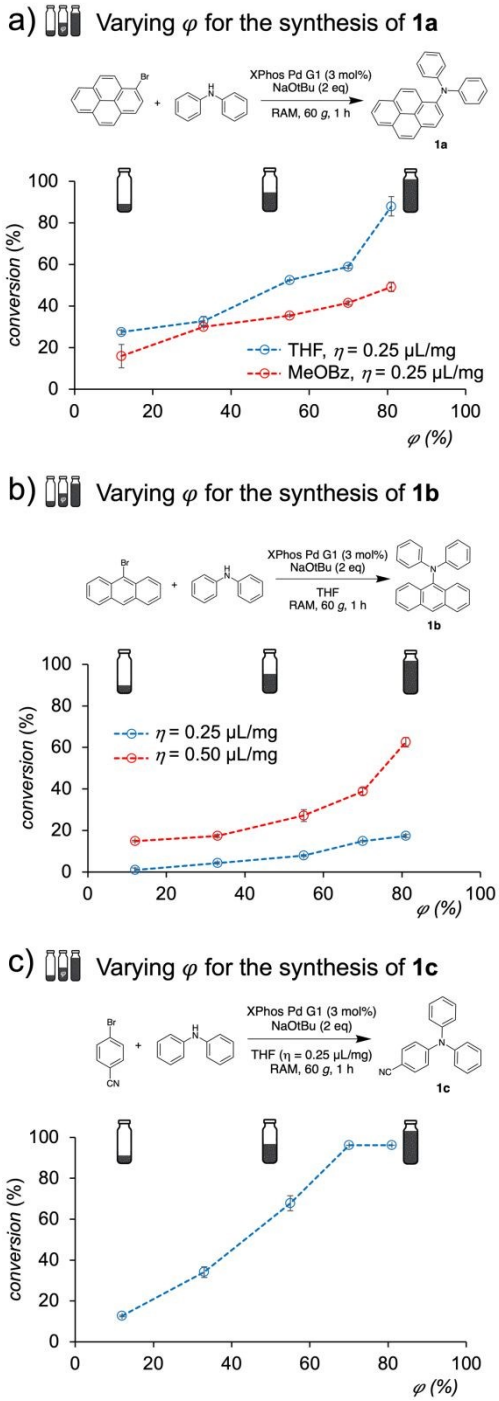

Fig. 2. Dependence of the Buchwald-Hartwig amination reactivity in RAM on the filling ratio (φ) for the coupling of a) 1-bromopyrene (solid) and diphenylamine (solid) to form **1a** in presence of THF or MeOBz (η = 0.25 µL/mg) as the liquid additive; b) diphenylamine and 9-bromoanthracene (solid) to form **1b** in presence of THF at different η-values (η = 0.25 and 0.50 µL/mg); c) diphenylamine (solid) with 4-bromobenzonitrile (solid) to give product **1c** in presence of THF (η = 0.25 µL/mg**)**. Corresponding plots with respect to reaction scale are shown in ESI Fig. S4. All φ values are approximate and correspond to the filling level of the initial reaction mixture, before the onset of RAM.

View Article Online
DOI: 10.1039/D6GC00784J

explored by ball-milling.[33] We conducted the RAM reactions using the LabRAM II instrument, typically in commercial 2.5 mL volume polypropylene vials. An equimolar mixture of reactants (0.25 mmol) in the presence of 3 mol% first-generation (G1) XPhos-Pd catalyst[37] and two equivalents of sodium *tert*-butoxide (NaO*t*Bu) base was subjected to RAM at 60 *g* for 60 minutes. Analysis of the crude reaction mixture by ^{1}H NMR after dissolution in $CDCl_3$ revealed no product formation, consistent with the previously reported lack of reactivity upon neat milling.[33] Next, we explored the effect of adding a small amount of liquid additive, in the η-range from 0 to 1.5 µL/mg. These conditions are consistent with those typically used in liquid-assisted mechanochemistry.[42,44] After 60 minutes of RAM at 60 *g* in the presence of tetrahydrofuran (THF), ^{1}H NMR analysis of the crude reaction mixture revealed a monotonic increase in conversion to **1a** with increasing η, reaching a plateau at ca. 50 % conversion (ESI Fig. S3).

However, increasing the reaction scale, without altering the size of the reaction vessel, led to a significant improvement in reactivity. The conversion was found to generally increase with respect to φ (Fig. 2a),[3,45] which was estimated by comparing the height of the reaction mixture in the vial before the RAM experiment to the height of the vial. While the initial experiments were performed at ca. φ = 10-15 %, increasing the filling ratio led to improved conversions, reaching ca. 90 % at a φ-value of ca. 80 %, based on ^{1}H NMR analysis after 60 minutes of RAM. To ensure that the analysis is not affected by sample preparation time, selected reactions were analysed by either first quenching the residual strong base using water, followed by extraction into $CDCl_3$, or by directly dissolving the reaction mixture in $CDCl_3$. Both methods of analysis gave comparable results (ESI Fig. S5). Overall, the aforementioned observations suggest φ as a previously not reported parameter to optimize reactions in RAM. It is worth noting that reactions by ball-milling generally perform worse with increased filling ratio,[3,45] as the additional material hinders the motion of milling media, reducing mixing and energy transfer. The improvement in reactivity by increasing the reactor volume occupied by reactants, therefore highlights a fundamental difference in reaction design between acoustic mixing and ball-milling.

To test the generality of using φ to modify reaction conversion, the coupling of diphenylamine was further explored with 9-bromoanthracene and 4-bromobenzonitrile, to give **1b** and **1c**, respectively (Fig. 2b,c). These reactions similarly showed a notable improvement in conversion with increasing φ. Similar behaviour was also seen when using a different liquid additive, methyl benzoate (MeOBz) (Fig. 2a), as well as when using different combinations of liquid and solid reactants such as *N*-methylaniline (liquid) with bromobenzene (liquid) or with 4-bromobenzonitrile (solid), respectively (ESI Fig. S6). The latter transformation was also attempted using alternative bases, such as KO*t*Bu, LiO*t*Bu and NaOMe, but gave poorer results (ESI Table S11). The use of MeOBz as the liquid additive (Fig. 2a) was of particular interest as an environmentally-friendly, high-boiling alternative (boiling point 200 °C) to THF (boiling point 66 °C), suitable for exothermic or elevated temperature reactions. While conversion for each of the explored reactions improved with φ, the dependence of conversion on filling ratio was in each case different, possibly reflecting the complexity of the still unclear relationship between filling ratio and mixing.[29,30] Overall, these results present φ as a parameter to design and control reactions under resonant acoustic mixing conditions.

Next, we explored how changes to acceleration affect reactivity, by conducting the synthesis of **1a** at 80 *g* and 100 *g*, resulting in ^{1}H NMR conversions of >95 % after ca. 15 and 10 minutes, respectively. This is a notable reduction in reaction time compared to 60 minutes previously reported for ball-milling in the presence of 5 mol% $Pd(OAc)_2$, tris(*tert*-butyl)phosphine and NaO*t*Bu.[33] The rapid reaction under RAM conditions led us to consider the potential importance of frictional heating on reactivity and, for this purpose, the opaque 2.5 mL volume polypropylene vessels were replaced with optically transparent commercial 5 mL volume borosilicate glass vials suitable for infrared temperature monitoring (thermography) using a forward-looking infrared (FLIR) camera (ESI Figs. S1, S2). Whereas no incidents were encountered in this work, it should be kept in mind that using glass vials could represent a hazard. To verify that the reactions conducted in 5 mL glass vials are consistent with those obtained in 2.5 mL polypropylene vials, selected reactions were conducted in both reactor types at approximately the same φ, showing overall similar results (ESI Table S12). Real-time evolution of the reaction temperature was initially monitored for the RAM synthesis of **1a** at 100 *g* and φ = 80 % (Fig. 3, ESI Fig. S10), over 60 minutes.

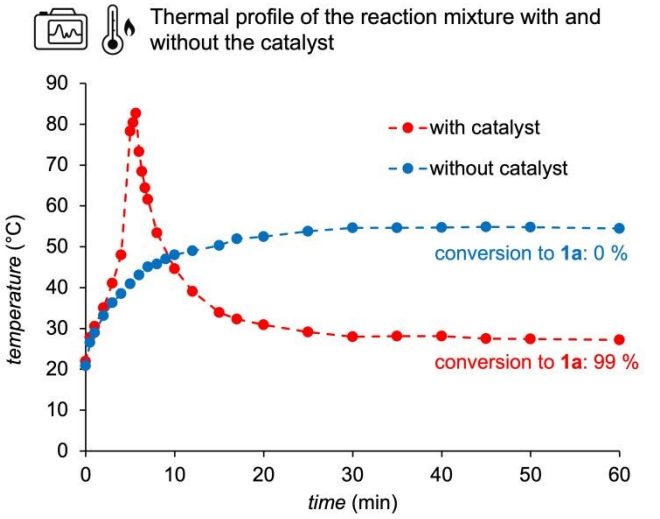

Fig. 3. Real-time measured thermal profile of the reaction mixture in the presence (3 mol%, red, full conversion) and absence (blue, no reaction) of palladium catalyst (Xphos-Pd-G1). Reaction conditions: diphenylamine (1 equivalent, 4.5 mmol), 1-bromopyrene (1 equivalent, 4.5 mmol), NaO*t*Bu (2 equivalents, 9 mmol), THF (η = 0.25 µL/mg), 100 *g*, $\varphi \approx$ 80%.

In the absence of the palladium catalyst, no reaction is observed, and thermographic monitoring showed a monotonic increase in temperature from ca. 20 °C to 50 °C over ca. 20 minutes, after which the temperature remained relatively constant. This measurement, conducted in duplicate,

View Article Online
DOI: 10.1039/D5GC00758H

provides a good estimate of frictional heating upon RAM at 100 *g* in the absence of Buchwald amination reaction. A very different temperature profile was observed, however, in the presence of 3 mol% palladium catalyst, revealing a short-lived (ca. 5-10 minutes) increase and decrease in temperature soon after initiating mixing, reaching a maximum of ca. 85 °C, and then rapidly falling to ca. 30 °C . We attribute the higher final temperature of the non-reactive system in the absence of a catalyst, compared to the reaction mixture in the presence of the catalyst, to both chemical, as well as rheological differences. On one hand, the system without the catalyst remained a thick paste that allowed for sustained frictional heating, while the reaction mixture in the presence of the catalyst underwent a change in chemical composition and became more solid, reducing the capacity for frictional heating. On the other, it is also likely that difference in heat capacities of the two reaction mixtures as a result of different chemical compositions once the reaction has taken place, plays a role.

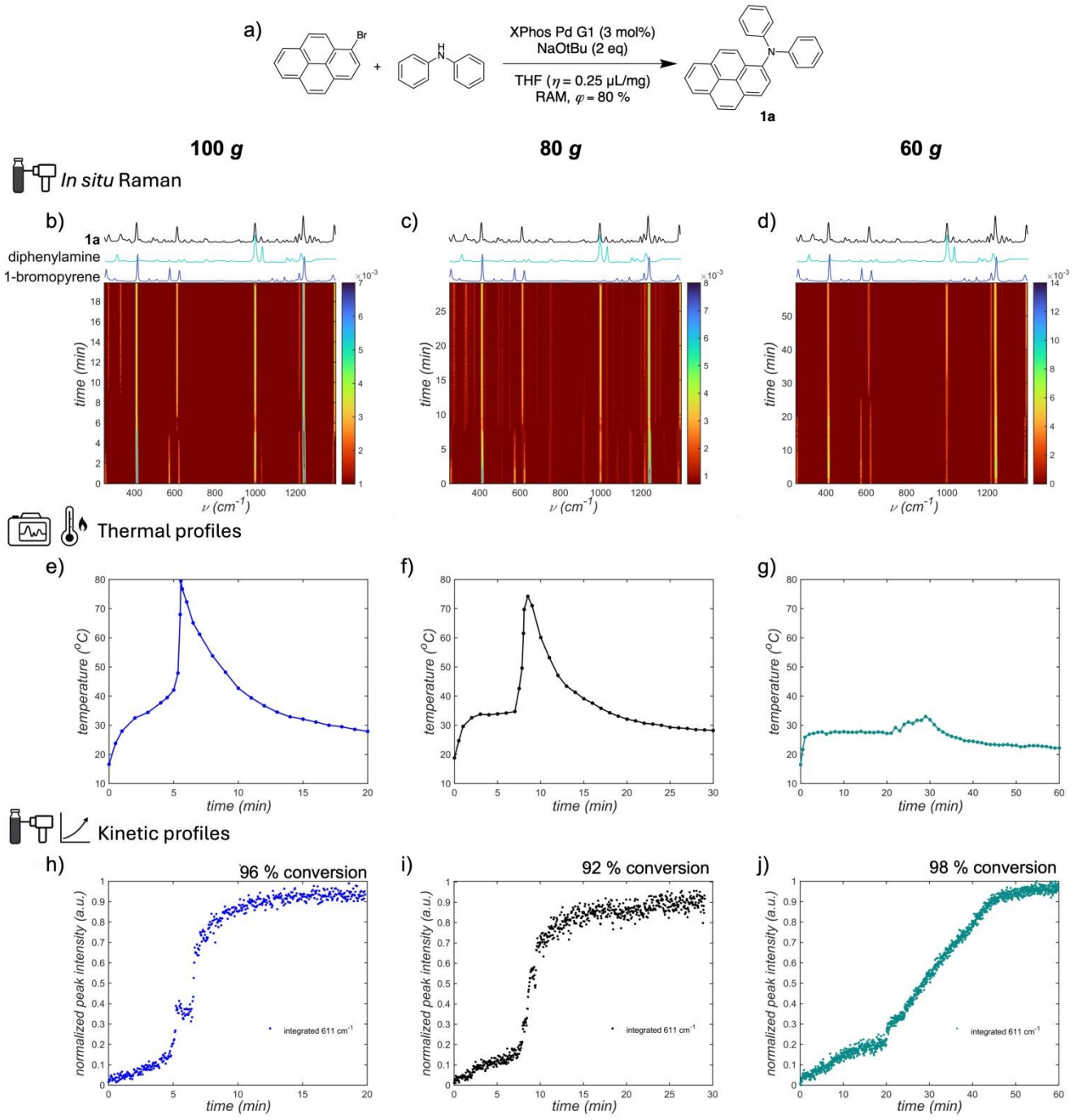

Fig. 4. Results of real-time thermal and Raman spectroscopy monitoring of the RAM Buchwald-Hartwig amination of 1-bromopyrene and diphenylamine to give **1a** at accelerations of 100 *g*, 80 *g*, and 60 *g*: a) reaction scheme, b-d) Raman spectroscopy time-resolved water-fall plot for the reaction run at b) 100 *g*, c) 80 *g* , and d) 60 *g* accelerations; e-g) *in situ* thermography data for reactions run at e) 100 *g*, f) 80 *g*, and g) 60 *g*; h-j) reaction profiles based on peak integration of Raman band at 611 cm^{-1} for reactions run at h) 100 *g*, i) 80 *g*, and j) 60 *g*. All reactions were conducted in triplicate (see ESI Figs. S10-12). Reaction conditions: diphenylamine (4.5 mmol), 1-bromopyrene (4.5 mmol), NaO*t*Bu (9 mmol), XPhos Pd G1 (3 mol%), THF (η = 0.25 µL/mg). The conversions were measured by ^{1}H NMR for the reaction mixtures dissolved immediately after the experiment.

View Article Online
DOI: 10.1039/D6GC00784H

ARTICLE

The appearance of exotherms during Buchwald-Hartwig reaction has been previously reported, and represents an important consideration for reaction scalability and safety.[26] Consequently, to further investigate the relationship between the appearance of the thermal spike and reaction conversion, the reaction was tracked in real time at accelerations of 60 *g*, 80 *g* and 100 *g* using simultaneous thermographic monitoring and Raman spectroscopy in both the fingerprint (200-1400 cm^{-1}) and low-frequency (THz, from the Rayleigh line to 200 cm^{-1})[46] regions. Whereas fingerprint Raman spectroscopy permits direct insight into reaction kinetics, monitoring in the THz-region was recently shown to also permit detecting the appearance and disappearance of bulk crystalline phases,[47] providing a route for simultaneous tracking of changes in molecular, as well as extended crystal structure of substances.[47,48] The ability to track the crystallinity of reaction components by benchtop THz-Raman spectroscopy, rather than by currently ubiquitous synchrotron X-ray diffraction, presents an exciting opportunity to gain insight into the phase behaviour of mechanochemical and/or solventless reactions, which has generally been limited to qualitative visual observations or calorimetric experiments.[49-52] To ensure reproducibility, each monitoring experiment was performed in triplicate (see ESI Figs. S10-12).

For reactions at 100 *g*, the temperature profile consistently revealed a sharp, short-lived temperature increase to ca. 80 °C within the first 6 minutes of RAM (Fig. 3,4, ESI Fig. S10). A similar, but lower, spike in temperature (up to ~75 °C) was observed within 10 minutes for the reactions conducted at 80 *g* (Fig. 4, ESI Fig. S11). At 60 *g*, however, the temperature maximum was much less pronounced, reaching no more than ca. 34 °C (Fig. 4, ESI Fig. S12). Raman spectroscopy enabled following the progress of the reaction in real time, by tracking the disappearance of reactant bands at 574 cm^{-1} and 621 cm^{-1} assigned to 1-bromopyrene, and the appearance of **1a** product bands at 611 cm^{-1} and 1395 cm^{-1}. Tracking the **1a** band at 611 cm^{-1} revealed that the reactions at 80 *g* and 100 *g* exhibit sigmoidal behaviour: in both cases, the formation of **1a** is initially slow with up to ca. 10 % conversion, but then advances rapidly around 5 minutes (for 100 *g*) or 8 minutes (for 80 *g*) of RAM. The rapid increase in conversion coincided well with the spike in reaction temperature (Fig. 4, ESI Figs. S10, S11), consistent with Buchwald-Hartwig coupling reactions being accelerated at elevated temperatures.[40,45] Subsequent analysis of the reaction mixtures by ^{1}H NMR indicated that at 100 *g* and 80 *g* the reactions are effectively complete after 10 and 15 minutes of RAM with ca. 96 % and 92 % reactant conversion, respectively. In contrast, Raman profiles of reactions conducted at 60 *g* showed a more linear reaction profile, with full conversion reached after ca. 1 hour (Fig. 4, also see ESI Fig. S12). Immediate analysis of the reaction mixture after 60 minutes of RAM showed 98 % conversion to **1a**. Overall, the reaction time required to reach quantitative conversion at 60 *g* is comparable to the previously reported ball-milling work,[33] but working at 80 *g* and 100 *g* led to significant reaction acceleration, shown to be associated with rapid, autogenous heating. The change from sigmoidal to linear kinetic behaviour is reminiscent of behaviour previously reported in ball-milling reactions, where decreasing the milling frequency results in a similar change from sigmoidal to apparently linear kinetics.[53]

Real-time THz-Raman monitoring revealed that the formation of crystalline **1a** is preceded by a loss of crystallinity of the reaction mixture. At 100 *g*, the THz-Raman spectrum of the reaction mixture lost the sharp features characteristic of crystalline 1-bromopyrene and diphenylamine within ca. 5 minutes (Fig. 5a,b), leaving only a single broad signal in the range from the Rayleigh line to ca. 75 cm^{-1}. A broad signal in THz-Raman spectroscopy is generally consistent with a non-crystalline environment.[54,55] Moreover, a similar THz-Raman signal is also observed upon melting a freshly prepared reaction mixture on a thermally controlled sample stage, without a liquid additive, indicating that the reaction environment in RAM prior to formation of crystalline **1a** resembles a melt (see ESI Figs. S16, S17). While liquid intermediate phases, such as eutectics, have been noted in solventless and mechanochemical reactions,[51,52] their behaviour has generally been described only in qualitative terms. In this case, however, non-negative least-squares (NNLS) fitting[47,53] (see ESI Section S1.8) of the THz-Raman spectra of each reaction component, including that of the non-crystalline intermediate, provides an opportunity to analyze the appearance of such phases in a more detailed fashion. The representative spectrum of the non-crystalline intermediate was selected from the real-time measurement (experimental frame 121, see Fig. 5c) and NNLS analysis indicated that the intermediate becomes increasingly prominent over ca. 5 minutes and then rapidly decays, concomitant with the appearance of THz-Raman bands characteristic of crystalline **1a**. Based on a non-quantitative relative spectral contribution analysis, the relative amount of crystalline **1a** appears to develop following a sigmoid curve, simultaneously with the formation of Raman bands characteristic of **1a** in the fingerprint-Raman region. Overall, these observations indicate that the reaction at 100 *g* is mediated by a non-crystalline phase from which the crystalline **1a** appears. This observation might also be of potential relevance to analogous ball-milling reaction designs. Comparing the real-time spectroscopic and thermal monitoring data for reactions conducted at 80 *g* or 100 *g* indicates that the

View Article Online
DOI: 10.1039/D6GC00784H

temperature spike is closely associated with a rapid, sigmoidal increase in product formation. This temperature increase almost completely disappears upon conducting the reaction at a lower acceleration of 60 *g*, with the reaction profile now appearing approximately linear. This observation suggests that one approach to control thermal and kinetic behaviour of reactions conducted by RAM is by varying acceleration. Alternatively, we also find that temperature increase in RAM can also be avoided by reducing *φ*. This is illustrated by conducting the reaction using the same amount of starting material (4.5 mmol), but in a glass vial of approximately double the volume (5 mL vs. 9 mL, see ESI Fig. S1) and similar internal diameter (13.2 mm vs. 14.7 mm, respectively), effectively reducing *φ* to ca. 40 %. The reaction exhibited a significantly smaller temperature increase, to ca. 35 °C (Fig. 6a), while reaction conversion after 60 minutes of RAM was found by ^{1}H NMR to be >95 %.

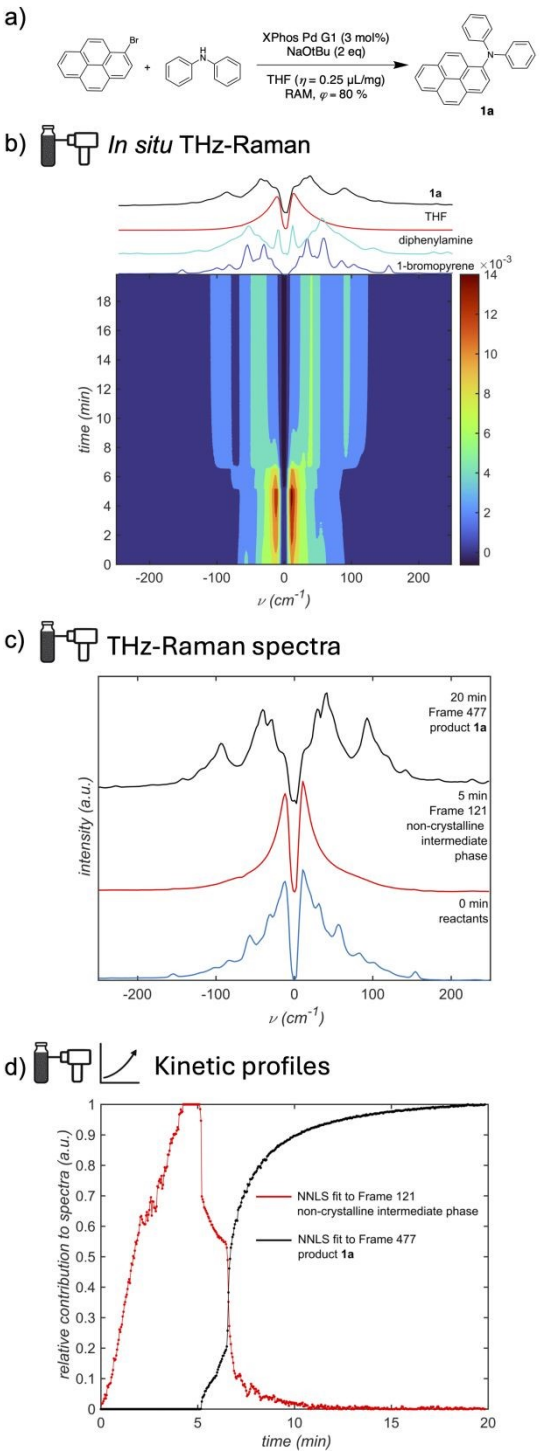

Fig. 5. Real-time THz-Raman monitoring of the RAM Buchwald-Hartwig amination of 1-bromopyrene and diphenylamine to form **1a** at 100 *g*: a) reaction scheme; b) time-resolved THz-Raman spectrum of the reaction; c) selected individual spectra (frames) collected after 0, 5 and 20 minutes of RAM, representing the spectra of the reactants, the non-crystalline intermediate and the product, that were used for NNLS fitting. d) Change in spectral contribution of the non-crystalline intermediate (red) and crystalline product **1a** (black), as established by NNLS fitting of THz-Raman spectra for the intermediate (representative spectrum is frame 121, collected at ~ 5 min, shown in panel 4b, red), and **1a** (representative spectrum is frame 477, collected at ~20 min, shown in panel 4b, black).

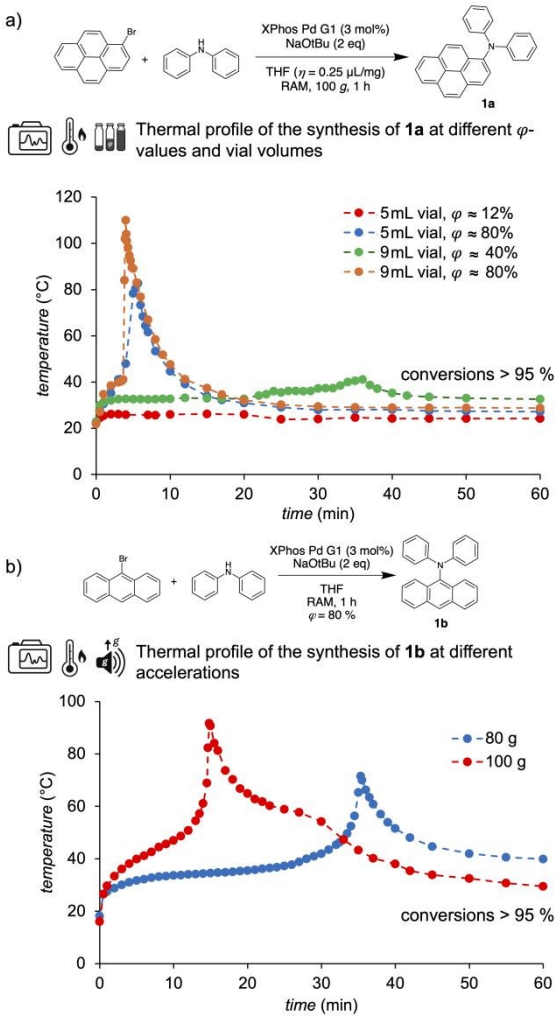

Fig. 6. Thermal monitoring data for the Buchwald-Hartwig coupling of diphenylamine with a)1-bromopyrene to form **1a** at 100 *g* at different *φ*-values (12, 40 and 80 %) and vial volumes (5 and 9 mL) and b) 9-bromoanthracene to form **1b** at accelerations of 80 *g* and 100 *g* (for *φ*≈80 %). All *φ* values are approximate and correspond to the filling level of the initial reaction mixture, before the onset of RAM.

Conversely, if both the volume of the reaction vial and the scale of the reaction are doubled, *i.e.*, maintaining the same initial *φ*-value (ca. 80 %), a short-lived temperature increase is again observed (90 to 110 °C) within 4 minutes (Fig. 6a). It is not yet

View Article Online
DOI: 10.1039/D6GC00784H

clear why changing φ, but using the same amount of material, influences reaction progress. Potential explanations might include general differences in mixing, differences in heat dissipation due to sample being more scattered across the reactor at low φ, or the reactor lid acting as a secondary transducer of mechanical energy to the reaction mixture at higher φ. We note that mixing under RAM conditions is an area of active study.[29,30]

A similar thermal profile at high acceleration was also observed for the coupling of 9-bromoanthracene and diphenylamine to form **1b**. At 100 *g* and 80 *g* (both at φ = 80 %) a temperature spike appeared, similar to what was observed for the synthesis of **1a**. However, this was only observed after approximately 15 minutes and 35 minutes of mixing at 100 *g* and 80 *g*, respectively (Fig. 6b, also ESI Fig. S18). Simultaneous real-time *in situ* monitoring of the synthesis of **1a** with THz-Raman spectroscopy suggests that the appearance of a thermal spike is not related to RAM-induced friction, but instead correlates with the reaction event. In such a scenario, the observed thermal signature would indicate that the coupling of diphenylamine with 9-bromoanthracene is already highly advanced after 15 minutes at 100 *g*. Indeed, analysis of the reaction mixture after 15 minutes by ^{1}H NMR spectroscopy revealed 74 % conversion to **1b**. Overall, the real-time measured thermal profiles reveal a significant temperature evolution in the Buchwald-Hartwig amination by RAM, related not to frictional heating but to the chemical transformation. This, together with the appearance of an induction period followed by a clear temperature spike, as opposed to a continuous increase in temperature, represents a behaviour similar to mechanically-induced self-propagating reactions (MSRs), typically observed in highly exothermic inorganic mechanochemical reactions.[56]

Having observed that higher φ and acceleration values lead to improved conversions to **1a** and **1b**, we explored whether such behaviour will be seen for a wider range of reactants (Table 1). A broader set of reactions were explored in triplicate both

Table 1. Comparison of the effectiveness of the Buchwald-Hartwig amination under different liquid-assisted RAM conditions, comparing conversion achieved after 10 minutes at 100 *g*, $\varphi \approx$ 80% to conversion achieved after 1 hour at 60 *g*, $\varphi \approx$12%. Conversions are based on triplicate experiments, through ^{1}H NMR analysis of crude reaction mixtures immediately after the RAM experiment.

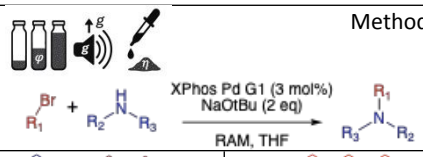

Method comparison for different φ-values, accelerations, η-values and reaction times

Conditions for $\varphi \approx$ 12 %: 60 *g*, 1 hour
Conditions for $\varphi \approx$ 80 %: 100 *g*, 10 minutes or a) 1 hour

	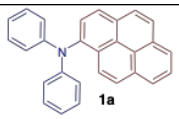 1a	 1b	 1c	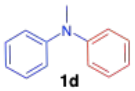 1d	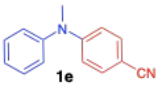 1e
$\varphi \approx$ 12 %	53 % ± 4 (η_{max} = 1.50 µL/mg) 30 % ± 2 (η = 0.25 µL/mg)	21 % ± 3 (η_{max} = 1.50 µL/mg) 17 % ± 2 (η = 0.50 µL/mg)	13 % ± 1 (η_{max} = 0.25 µL/mg)	99 % ± 0 (η_{max} = 0.25 µL/mg) 96 % ± 1 (η = 0.00 µL/mg)	13 % ± 2 (η_{max} = 0.25 µL/mg)
$\varphi \approx$ 80 %	96 % ± 1 (η = 0.25 µL/mg)	98 % ± 1 (η = 0.50 µL/mg)[a]	87 % ± 2 (η = 0.25 µL/mg)	92 % ± 1 (η = 0.00 µL/mg)	96 % ± 1 (η = 0.25 µL/mg)
	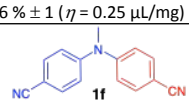 1f	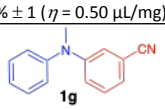 1g	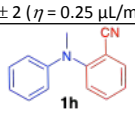 1h	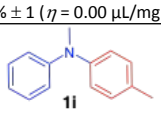 1i	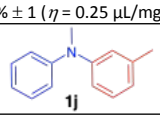 1j
$\varphi \approx$ 12 %	7 % ± 1 (η_{max} = 0.37 µL/mg) 4 % ± 1 (η = 0.25 µL/mg)	70 % ± 3 (η_{max} = 0.50 µL/mg) 58 % ± 4 (η = 0.25 µL/mg)	70 % ± 2 (η_{max} = 0.50 µL/mg) 54 % ± 3 (η = 0.25 µL/mg)	99 % ± 0 (η_{max} = 0.75 µL/mg) 92 % ± 1 (η = 0.00 µL/mg)	99 % ± 0 (η_{max} = 0.00 µL/mg)
$\varphi \approx$ 80 %	48 % ± 3 (η = 0.25 µL/mg)[a]	87 % ± 3 (η = 0.25 µL/mg)	93 % ± 1 (η = 0.25 µL/mg)	87 % ± 1 (η = 0.00 µL/mg)	94 % ± 2 (η = 0.00 µL/mg)
	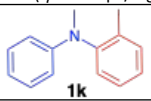 1k	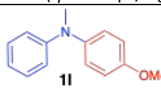 1l	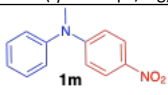 1m	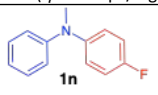 1n	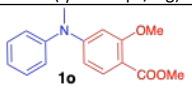 1o
$\varphi \approx$ 12 %	99 % ± 0 (η_{max} = 1.00 µL/mg) 55 % ± 3 (η = 0.00 µL/mg)	99 % ± 0 (η_{max} = 0.50 µL/mg) 60 % ± 4 (η = 0.00 µL/mg)	96 % ± 2 (η_{max} = 0.75 µL/mg) 83 % ± 3 (η = 0.25 µL/mg)	99 % ± 0 (η_{max} = 0.25 µL/mg)	79 % ± 4 (η_{max} = 1.50 µL/mg) 58 % ± 5 (η = 0.25 µL/mg)
$\varphi \approx$ 80 %	93 % ± 0 (η = 0.00 µL/mg)	95 % ± 2 (η = 0.00 µL/mg)	95 % ± 1 (η = 0.25 µL/mg)	91 % ± 2 (η = 0.25 µL/mg)	81 % ± 5 (η = 0.25 µL/mg)
	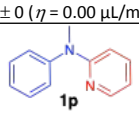 1p	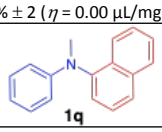 1q	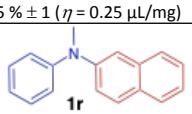 1r	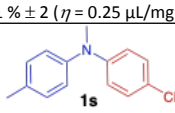 1s	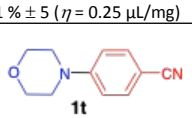 1t
$\varphi \approx$ 12 %	88 % ± 3 (η_{max} = 0.75 µL/mg) 60 % ± 5 (η = 0.00 µL/mg)	98 % ± 1 (η_{max} = 0.50 µL/mg) 94 % ± 2 (η = 0.25 µL/mg)	97 % ± 1 (η_{max} = 0.37 µL/mg) 88 % ± 3 (η = 0.25 µL/mg)	99 % ± 0 (η_{max} = 0.25 µL/mg)	27 % ± 5 (η_{max} = 0.37 µL/mg) 25 % ± 3 (η = 0.25 µL/mg)
$\varphi \approx$ 80 %	91 % ± 2 (η = 0.00 µL/mg)	94 % ± 2 (η = 0.25 µL/mg)	85 % ± 2 (η = 0.25 µL/mg)	95 % ± 2 (η = 0.25 µL/mg)	44 % ± 10 (η = 0.25 µL/mg)[a]

a) reaction conducted for 60 minutes at 100 *g*. All experiments were done in triplicate and NMR analysis was carried out immediately after RAM either by dissolving approximately one-half of the sample in DMSO-d_6 to which a small amount of water was added to quench the residual strong base NaO*t*Bu (**1d**, **1f**-**1l** and **1n**-**1t**), or by quenching with water, followed by rapid extraction into $CDCl_3$ (**1a**-**1c**, **1e**, **1m**), depending on product solubility. To ensure that the reaction does not noticeably proceed during NMR analysis, the spectrum for the synthesis of **1a** was measured immediately after RAM ($\varphi \approx$ 12 %, 1 h, 60 *g*), and then again after ca. 1 hour, without any significant change. For all compounds, η-screening was performed in the 0–1.5 µL mg^{-1} range under standard conditions (1 hour, 60 *g*, φ = 12 %), and the conversions at η_{max}[4,6] are reported in the Table.

View Article Online
DOI: 10.1039/D6GC00784H

under the highly effective conditions of 100 *g*, $\varphi \approx 80$ %, and under the initially explored conditions of 60 *g*, $\varphi \approx 12$ %, that would be somewhat similar to those found in a ball-milling design. Moreover, we have also explored how the reaction conversion at 60 *g*, $\varphi \approx 12$ % changes with η, allowing us to determine the η-value at which the conversion reaches a maximum (η_{max}).[4,6] This enabled also the comparison of reactivity at 60 *g*, $\varphi \approx 12$ % under η-optimized conditions, to reactivity at 100 *g*, $\varphi \approx 80$ % and a set, non-optimized small η-value. The results (Table 1), in almost all cases, show 80 % to 90 % conversions within 10 minutes of RAM at 100 *g* and $\varphi \approx 80$ %. Importantly, these conditions permitted high-yielding reactions to be readily achieved without extensive η screening, with the amount of liquid additive simply set in the range 0.25-0.50 µL/mg. For **1b**, a longer time of 60 minutes was needed to obtain high reactant conversions (>95 %), while for **1f** and the aliphatic amine morpholine (**1t**), the conversion remained in the 40 % range. In contrast, reactions conducted at 60 *g*, $\varphi \approx 12$ %, either at the same η-value or at η_{max}, resulted in generally worse conversions even after one hour. For example, conversion to **1a** ($\eta = 0.25$ µL/mg) was only 30 % ± 2 after 1 hour (Fig. 6a, Tab. 1).

With a clearer understanding of RAM reaction parameters, we next explored increasing the reaction scale to 100 mmol (total weight 66.5 g) for the synthesis of **1a** (Fig. 7). The 22-fold increase in reaction scale (from initially 4.5 mmol, total weight 3.9 g) was performed by adjusting the quantity of all materials accordingly and using a 100 mL vessel (see ESI Figs. S1, S7). Considering the potential of exothermic behaviour revealed by smaller-scale *in situ* measurements, the reaction was conducted in a borosilicate jar capable of withstanding temperatures of up to 150 °C. Real-time monitoring of the reaction at 60 *g*, with initial φ at ca. 70 % and η-value of 0.25 µL/mg revealed the appearance of an exotherm reaching up to 85 °C within 6 minutes, with Raman spectroscopy indicating that the reaction should be essentially complete within ca. 15 minutes (Figs 7b, d, f). Subsequent analysis of the reaction mixture after a total of 60 minutes RAM, by sampling at five different locations in the reaction jar, demonstrated almost complete conversion (98 % for all sections), which was also confirmed by a repeat experiment (conversion in the range 94 % - 95 % for six sections of the sample). Overall, increasing the reaction scale led to an increase in reaction kinetics compared to experiments at 4.5 mmol level, which is probably related to less efficient cooling of the larger reaction mixture.

According to real-time Raman spectroscopy data and subsequent NMR analysis (Fig. 7b,d,f), the increased reaction kinetics at a 100 mmol scale enabled the reaction to be completed within 15 minutes using 3 mol% catalyst. This significantly exceeds the size and speed of the previously reported LAG ball-milling approach, and confirms the potential of RAM-based reactions for scale-up without bulk solvents.[3,15] Encouraged by this result, we also explored the reaction at 100 mmol scale using 1 mol% amount of catalyst (Fig. 7c, e, g). Reducing the amount of catalyst still led to almost complete conversion to **1a**, although within ca. 80 minutes, as indicated by real-time Raman spectroscopy, and subsequent NMR analysis. Specifically, the reaction at 1 mol% catalyst and 100 mmol scale exhibited an extended period of reaction activation, with an exothermic signal appearing only at ca. 40 minutes into the RAM process, concomitant with a sigmoidal increase in reaction progress. We note that the total power consumption of the RAM instrument may vary depending on the acceleration. Power consumption tests conducted using an equivalent weight of sand indicate that operating a 100 mmol reaction at 60 *g* consumes ca. 39% less power (103 W) compared to an analogous process at 100 *g* (169 W). In context of reaction design this suggests that longer reaction times at lower accelerations might be partially offset by lower power requirements.

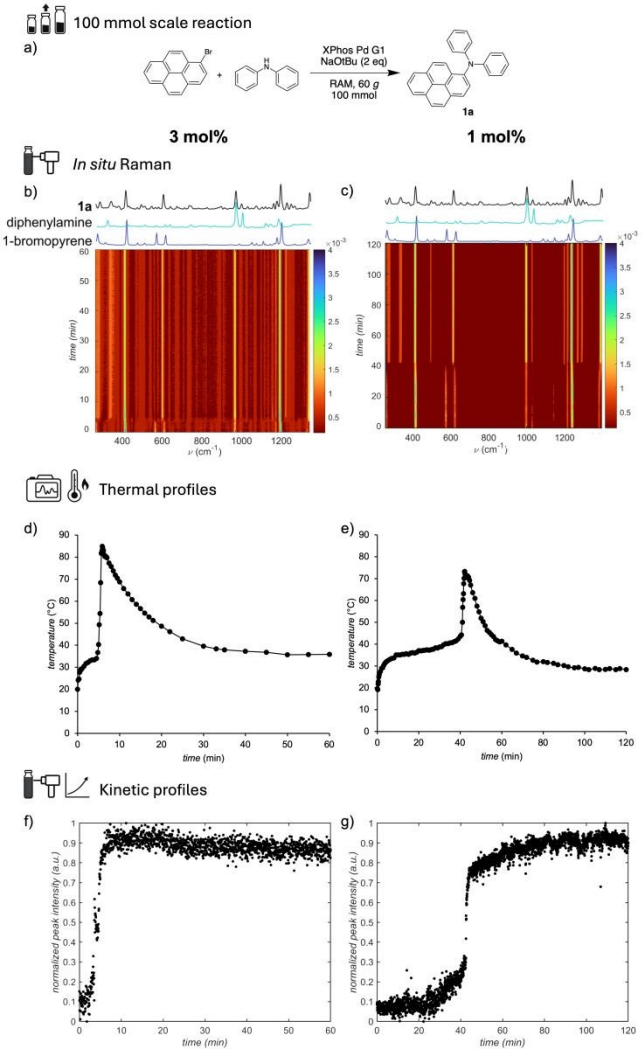

Fig. 7. Results of real-time thermal and Raman spectroscopy monitoring of the a) 100 mmol scale RAM Buchwald-Hartwig amination of 1-bromopyrene and diphenylamine to give **1a** using either 3 or 1 mol% of XPhos Pd G1 at acceleration of 60 *g*: b,c) Raman spectroscopy time-resolved water-fall plot for the reaction run with. b) 3 mol% and c) 1 mol% of catalyst; d,e) *in situ* thermography data for reactions run with d) 3 mol% and e) 1 mol% of XPhos Pd G1; f,g) reaction profiles based on peak integration of Raman band at 611 cm^{-1} for reactions run with f) 3 mol% and g) 1 mol%. Reaction conditions: diphenylamine (4.5 mmol), 1-bromopyrene (4.5 mmol), NaO*t*Bu (9 mmol), XPhos Pd G1 (3 or 1 mol%), THF ($\eta = 0.25$ µL/mg), $\varphi \approx 70$ %.

View Article Online
DOI: 10.1039/D5GC00784H

In order to estimate the maximum temperature (maximum adiabatic change in temperature, ΔT_{AD}) that could be reached during the RAM-based Buchwald-Hartwig coupling reaction, we conducted a set of DSC experiments to measure the heat released (Q) and the heat capacity of the reaction mixture (C_p). The ratio of these values is expected to provide ΔT_{AD},[57] and similar approaches have previously been used to evaluate the potential of MSRs for self-ignition.[56,58] While the details of the experiments and calculations are provided in the ESI (Sections S1.6 and S8), it is important to note that, compared to reactions in homogeneous solution, evaluation of the ΔT_{AD} for a liquid-assisted reaction system is complicated by the exothermic signal of the reaction being affected by endothermic processes, such as the melting of reactants or their dissolution in the small amount of liquid additive, as well as by the C_p of the reaction mixture changing due to change in composition or state of aggregation. With these limitations in mind, the DSC analyses indicated a ΔT_{AD} value in the range of 90 °C-110 °C. Estimating that frictional heating could increase the initial reaction mixture temperature to ca. 50 °C (Fig. 3), such a ΔT_{AD} value indicates that the reaction could reach maximum temperatures in the range of 140-160 °C. Whereas borosilicate glass used in present real-time monitoring experiments is expected to withstand temperatures to ca. 150 °C, and herein monitored small-scale reactions have not been observed to reach temperatures greater than 110 °C, the estimated ΔT_{AD} indicates that further scaling-up is likely to require the use of vessels of greater temperature and pressure robustness, with liquid additives of higher boiling points such as MeOBz being preferred to THF. Most importantly, the estimated ΔT_{AD} is consistent with previous observations of exothermicity in Buchwald-Hartwig aminations,[26] and highlights the importance of the herein explored strategies to control the reaction kinetics and thermal behavior of the reaction using the RAM setup (for example, by modifying φ and/or acceleration).

Finally, the potential for stoichiometric selectivity in the RAM-based Buchwald-Hartwig aminations was explored through reactions of the primary amine 3,5-dimethoxyaniline with one or two equivalents of an aryl bromide (Fig. 8a). Notably, such an approach to triarylamines was recently explored under ball-milling conditions, requiring external heating.[43] We conducted the reactions using one equivalent of either 3-bromotoluene (a liquid) or 4-bromobenzonitrile (a solid) as the aryl bromide, in the presence of two equivalents of NaO*t*Bu, and methyl benzoate (MeOBz) as the liquid additive (η = 0.5 µL/mg), initially at $\varphi \approx 12$ % and an acceleration of 60 g. After 1 hour of RAM, reactions with one equivalent of the aryl bromide showed complete conversion to the expected bis-arylated[59] coupling products **1u** or **1v**. Increasing the acceleration to 100 g and φ to ca. 95 %, greatly accelerated the synthesis, resulting in 98 % conversion to **1u** or **1v** after 10 minutes.

Conducting the reactions using two equivalents of the aryl bromide and four equivalents of NaO*t*Bu, however, yielded only **1u** or **1v** at $\varphi \approx 12$ %, after 1 hour of RAM at 60 g. The targeted 1:2 coupling products could be obtained by modifying φ, acceleration, and the η-value. Specifically, screening the reaction of 3-bromotoluene at different φ-values, while maintaining an acceleration of 100 g and η = 0.25 µL/mg, revealed that lower filling ratios result in the bis-arylated **1u**, whereas higher φ led to an increased amount of the triarylamine **1w** (Fig. 8b). After two hours of RAM, analysis of the reaction conducted at 100 g and $\varphi \approx 80$ % revealed the formation of **1w** and **1u** in an approximate 74:26 ratio, with no residual 3,5-dimethoxyaniline, assessed by ^{1}H NMR spectroscopy. Similar behaviour was observed with 4-bromobenzonitrile (Fig. 8c).

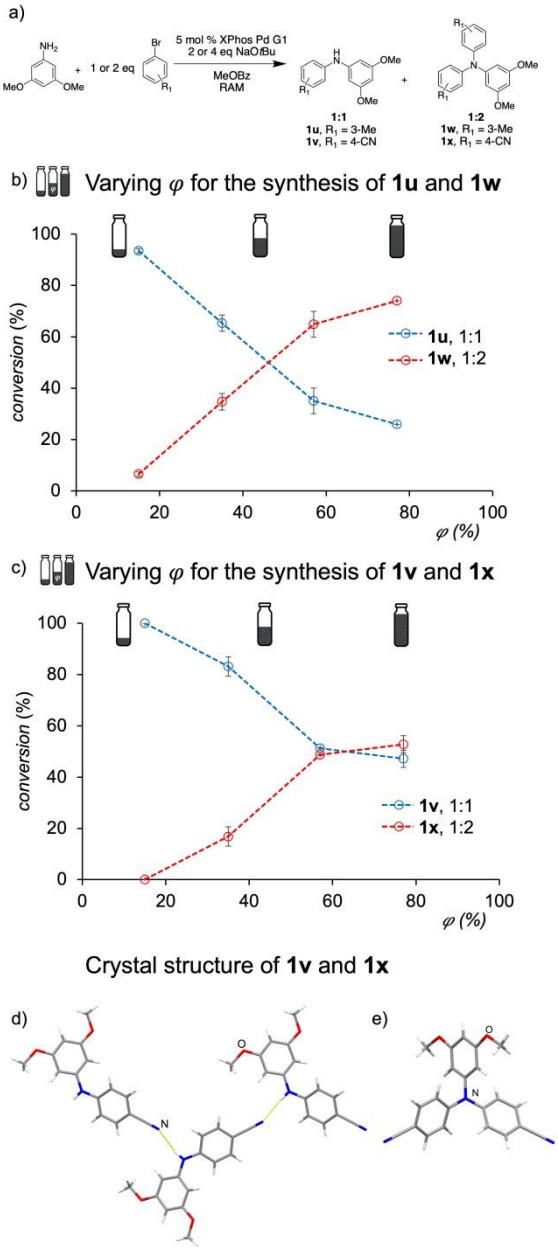

Fig. 8. Stoichiometric selectivity of the Buchwald-Hartwig amination reaction using RAM: a) the model coupling reaction and b) the φ-dependent formation of the 1:1 or 2:1 coupling products with 3,5-dimethoxyaniline following RAM at 100 g for 2 hours with MeOBz as liquid additive for 3-bromotoluene at η = 0.25 µL/mg, and c) for 4-bromobenzonitrile at η = 0.75 µL/mg. d) A chain of molecules held by N-H···N hydrogen bonds (yellow dotted lines) in the crystal structure of **1v** and e) a single molecule of **1x**, as established by single crystal X-ray diffraction structure analysis. Corresponding plots with respect to reaction scale are shown in the SI.

View Article Online
DOI: 10.1039/D6GC00784H

While **1v** was the only product observed after 2 hours of RAM at 100 *g* and φ = 12 %, performing the reaction at $\varphi \approx 80$ % led to the formation of the triarylamine **1x** in a 53:47 ratio with respect to the diarylamine **1v**, with no residual 3,5-dimethoxyaniline, based on ^{1}H NMR analysis. Formation of **1v** and **1x** was also confirmed by single crystal X-ray diffraction structure analysis of crystals grown by vapor diffusion of hexanes into a THF solution of the purified products (Fig. 8d,e).

Interestingly, comparing the RAM reactivity of 3,5-dimethoxyaniline and two equivalents of 3-bromotoluene or 4-bromobenzonitrile with a more conventional reaction design, *i.e.*, stirring (600 rpm) in a concentrated MeOBz environment (η = 5.0 µL/mg) at room temperature, resulted in quantitative conversion to only the bis-arylated products **1u** or **1v**, after 10 minutes and 90 minutes, respectively. Increasing the temperature led to the observation of the triarylamines **1w** and **1x**: after 2 hours at 45 °C **1w** and **1x** were observed in 7 % and 11 % conversions, respectively, while at 80 °C the reaction after 20 minutes progressed to conversions of **1w** and **1x** of 13% and 29%, respectively, and then stalled possibly due to catalyst degradation (see ESI Fig. S42).

Conclusions

This work establishes experimentally accessible parameters for the design and optimization of reactivity under Resonant Acoustic Mixing (RAM) conditions, and advances the understanding of such processes through real-time insight into the temperature evolution, reaction kinetics and bulk phase transformations. Using the Buchwald-Hartwig reaction as a model system, we have combined systematic screening with integrated real-time *in situ* monitoring of temperature, kinetics and bulk phase transformations, to establish how the amount of liquid additive, filling ratio (φ), and acceleration (*g*) govern reaction behaviour in RAM. We report a clear dependence of the reaction conversion on the filling ratio, as well as the ability to modify the reaction kinetics and the associated reaction thermal profile, by varying φ and/or the acceleration. The simultaneous use of real-time infrared thermography and *in situ* fingerprint and THz-Raman spectroscopies provides insight into the relationship between reaction profile and temperature evolution, and enables the detection of a non-crystalline, melt-like intermediate phase without requiring synchrotron X-ray diffraction or having to stop and visually inspect the reaction system. Application of NNLS analysis permitted this non-crystalline intermediate to be tracked and related to the formation of the crystalline Buchwald-Hartwig coupling product. Overall, variation of acceleration and φ enables tuning of reactivity to enable either near-quantitative conversions rapidly, often within 10-15 minutes, notably faster than previously reported ball-milling approaches.[33] The reactivity is also influenced by the reaction scale, most likely due to the exothermic nature of the herein explored Buchwald-Hartwig coupling, which enabled a model reaction to be conducted at a 100 mmol scale within ca. 15 minutes and at near-quantitative conversion.

The presented benchtop methodology for real-time *in situ* monitoring of RAM processes, that simultaneously provides information on reaction temperature, progress of a covalent bond-formation, and on the appearance and transformations of bulk crystalline or non-crystalline phases, contributes to the emergence of increasingly multi-pronged methods for real-time observation of mechanochemical reactivity.[27,28,60,61] The importance of such real-time studies is evident from the detection of short-lived temperature spikes during Buchwald-Hartwig coupling process at high accelerations, that resemble MSR behaviour observed in inorganic systems.[58,62] The observation of thermal spikes and the herein presented development of strategies to mitigate them by varying the acceleration or the reaction filling ratio, is expected to guide the design of RAM-based reactions, and most likely also other mechanochemical or solventless reaction strategies,[37,38] in such a way to ensure they are not only efficient, but also safer.[26,63] Indeed, understanding of how reactivity and heat transfer depend on RAM operating parameters is likely to be of particular importance when considering potential scale-up of RAM processes to large batch-based or even continuous designs,[1] as evidenced here by changes in thermal behaviour upon increasing reaction scale from 4.5 mmol to a 100 mol. Finally, the combined use of fingerprint and low-frequency Raman spectroscopy monitoring is anticipated to facilitate the mechanistic understanding of mechanochemical reactions in which the role of eutectic formation is unclear, such as in the previously proposed "hidden eutectic" reaction systems.[52]

Conflicts of interest

There are no conflicts to declare.

Data availability

Details of experimental procedures, along with characterization data, as well as NMR and THz-Raman spectra, thermal monitoring plots and X-ray crystallography information, in PDF format. Also included are crystallographic data in CIF format, which can also be obtained on request free of charge from the Cambridge Crystallographic Data Centre (CCDC), deposition numbers 2372358 and 2372359. The authors have cited additional references within the Supporting Information.[64-67]

Acknowledgements

We thank the support of Genentech, Inc., University of Birmingham, Leverhulme Trust (TF, THB), and NSERC CGS-D Scholarship (CBL). Prof. Duncan L. Browne, University College London, is acknowledged for valuable discussions. Dr. Jason Stafford, School of Chemical Engineering, University of Birmingham is acknowledged for providing access to the thermal camera, Dr. Mike Jenkins, School of Metallurgy & Materials, University of Birmingham, is acknowledged for access to the DSC. We thank Drs. Paul Clarke and Tim Mann, Perkin Elmer, for help in heat capacity measurements. LG would

View Article Online DOI: 10.1039/D5GC00784H

like to dedicate this work to the loving memory of her mother, Sylvie Gonnet, whose strength and support are a continuous inspiration.

Notes and references

1 C. J. Wright, P. J. Wilkinson, S. E. Gaulter, D. Fossey, A. O. Burn, P. P. Gill, *Propel. Expl. Pyrotech.* 2022, **47**, e202100146. DOI:10.1002/prep.202100146.

2 D. J. am Ende, S. R. Anderson, J. S. Salan, *Process Res. Dev.* 2014, **18**, 331–341. DOI:10.1021/op4003399.

3 L. Gonnet, C. B. Lennox, J.-L. Do, I. Malvestiti, S. G. Koenig, K. Nagapudi, T. Friščić, *Angew. Chem. Int. Ed.* 2022, **61**, e202115030. DOI:10.1002/anie.202115030.

4 M. Wohlgemuth, S. Schmidt, M. Mayer, W. Pickhardt, S. Grätz, L. Borchardt, *Chem. Eur. J.* 2023, **29**, e202301714. DOI:10.1002/chem.202301714.

5 F. Effaty, L. Gonnet, S. G. Koenig, K. Nagapudi, X. Ottenwaelder, T. Friščić, *Chem. Commun.* 2023, **59**, 1010-1013. DOI:10.1039/D2CC06013B.

6 a) L. Gonnet, C. B. Lennox, T. H. Borchers, J. Vainauskas, Y. Teoh, H. M. Titi, C. J. Barrett, S. G. Koenig, K. Nagapudi, T. Friščić, *Faraday Discuss.* 2023, **241**, 128-149. DOI: 10.1039/D2FD00131D; b) C. Spula, P. M. Preuß, L. Borchardt and S. Grätz, *Chem. Eur. J.* 2025, **31**, e202501137; c) J. D. Thorpe, J. Marlyn, S. G. Koenig and M. J. Damha, *RSC Mechanochem.* 2024, **1**, 244-249; d) C. B. Lennox, T. H. Borchers, L. Gonnet, C. J. Barrett, S. G. Koenig, K. Nagapudi, and T. Friščić, *Chem. Sci.* 2023, **14**, 7475-7481.

7 H. M. Titi, J.-L. Do, A. J. Howarth, K. Nagapudi, T. Friščić, *Chem. Sci.* 2020, **11**, 7578–7584. DOI:10.1039/D0SC00333F.

8 E. Hamzehpoor, F. Effaty, T. H. Borchers, A. Wahrhaftig-Lewis, X. Ottenwaelder, T. Friščić, D. F. Perepichka, *Angew. Chem. Int. Ed.* 2024, e202404539. DOI:10.1002/anie.202404539.

9 S. Hutsch, A. Leonard, S. Graetz, M. V. Hoefler, T. Gutmann, L. Borchardt, *Angew. Chem. Int. Ed.* 2024, e202403649. DOI: 10.1002/anie.202403649.

10 A. Nari, J. S. Ovens, D. L. Bryce, *RSC Mechanochem.* 2024, **1**, 50-62. DOI: 10.1039/D3MR00028A.

11 S. Nagapudi, K. Nagapudi, *Phys. Chem. Chem. Phys.* 2024, **26**, 12545-12551. DOI: 10.1039/D3CP04713J.

12 D. J. Eyckens, D. J. Hayne, L. C. Henderson, S. C. Howard, T. J. Raeber, R. Simons, A. L. Wilde, D. Yalcin, B. W. Muir, *Appl. Surf. Sci.* 2024, **646**, 158865. DOI: 10.1016/j.apsusc.2023.158865

13 K. Nagapudi, E. Y. Umanzor, C. Masui, *Int. J. Pharm.* 2017, **521**, 337–345. DOI: 10.1016/j.ijpharm.2017.02.027.

14 S. R. Anderson, D. J. am Ende, J. S. Salan, P. Samuels, Preparation of an Energetic-Energetic Cocrystal Using Resonant Acoustic Mixing. *Propellants, Explosives, Pyrotechnics* 2014, **39**, 637–640. DOI: 10.1002/prep.201400092.

15 a) D. Kong, L. Yi, A. Nanni, M. Rueping, *Nat. Commun.* 2025, **16**, 3983. DOI: 10.1038/s41467-025-59358-1; b) J. Marlyn, O. Del Carlo, J. D. Thorpe, M. J. Damha, *Green Chem.* 2025, **27**, 8313-8318. DOI: 10.1039/d5gc01768h; c) A. Nanni, D. Kong, C. Zhu, M Rueping, *Green Chem.* 2024, **26**, 8341–8347. DOI: 10.1039/D4GC01790K.

16 J. G. Osorio, E. Hernández, R. J. Romañach, F. J. Muzzio, *Powder Technol.* 2016, **297**, 349–356. DOI: 10.1016/j.powtec.2016.04.035

17 J. G. Osorio, K. Sowrirajan, F. J. Muzzio, *Adv. Powder Tech.* 2016, **27**, 1141-1148. DOI: 10.1016/j.apt.2016.03.025.

18 J. G. Osorio, F. J. Muzzio, *Powder Tech.* 2015, **278**, 46-56. DOI: 10.1016/j.powtec.2015.02.033.

19 A. J. Claydon, A. N. Patil, S. Gaulter, G. Kister, P. P. Gill, *Chem. Eng. Proc.* 2022, **173**, 108806. DOI: 10.1016/j.cep.2022.108806.

20 A. A. L. Michalchuk, K. S. Hope, S. R. Kennedy, M. V. Blanco, E. V. Boldyreva, C. R. Pulham. *Chem. Commun.* 2018, **54**, 4033-4036. DOI: 10.1039/c8cc02187b.

21 A. A. L. Michalchuk, E. V. Boldyreva, A. M. Belenguer, F. Emmerling, V. V. Boldyrev. *Front. Chem.* 2021, **9**. DOI: 10.3389/fchem.2021.685789.

22 O. Galant, G. Cerfeda, A. S. McCalmont, S. L. James, A. Porcheddu, F. Delogu, D. E.Crawford, E. Colacino, S. Spatari, *ACS Sustainable Chem. Eng.* 2022, **10**, 1430–1439. DOI: 10.1021/acssuschemeng.1c06434.

23 M. Lavayssiere, F. Lamaty, *Chem. Commun.* 2023, **59**, 3439–3442. DOI: 10.1039/D2CC06934B.

24 P. Ruiz-Castillo, S. L. Buchwald, *Chem. Rev.* 2016, **116**, 12564–12649. DOI: 10.1021/acs.chemrev.6b00512.

25 J. Magano, J. R. Dunetz, *Chem. Rev*. 2011, **111**, 2177–2250. DOI: 10.1021/cr100346g.

26 a) Q. Yang, N. R. Babij, S.; Good, *Org. Proc. Res. Dev*. 2019, **23**, 2608–2626. DOI: 10.1021/acs.oprd.9b00377 ; b) N. Marion, O. Navarro, J.; Mei, E. D. Stevens, N. M. Scott, S. P. Nolan, *J. Am. Chem. Soc*. 2006, **128**, 4101–4111. DOI: 10.1021/ja057704z ; c) O. Navarro, N. Marion, J. Mei, S. P. Nolan, *Chem. Eur. J.* 2006, **12**, 5142–5148. DOI: 10.1002/chem.200600283; d) O. P. Schmidt, D. G.; Blackmond, *ACS Catal*. 2020, **10**, 8926–8932. DOI: 10.1021/acscatal.0c01929.

27 a) H. Kulla, M. Wilke, F. Fischer, M. Röllig, C. Maierhofer, F. Emmerling, *Chem. Commun.* 2017, **53**, 1664-1667. DOI: 10.1039/c6cc08950j; b) S. Krause Hinojosa, T. Dogan, S. Fabig, S. Grätz and L. Borchardt, *Chem. Eur. J.* 2025, **31**, e01336.

28 a) H. Kulla, S. Haferkamp, I. Akhmetova, M. Röllig, C. Maierhofer, K. Rademann, F. Emmerling, *Angew. Chem. Int. Ed.* 2018, **57**, 5930-5933. DOI: 10.1002/anie.201800147; b) K. Užarević, N. Ferdelji, T. Mrla, P. A. Julien, B. Halasz, T. Friščić, I. Halasz, *Chem. Sci.* 2018, **9**, 2525-2532. DOI: 10.1039/c7sc05312f.

29 a) H. Sezer, D. Werner, J. A. Sykes, N. Bazin, P. Bolton, C. R. K. Windows-Yule, *Chem. Eng. Sci.* **2025**, **306**, 121166. DOI: 10.1016/j.ces.2024.121166; b) S. Zhang, X. Wang, L. Zhang, *Powder Technol*. 2025, **456**, 120841. DOI: 10.1016/j.powtec.2025.120841.

30 L. Vugrin, C. Chatzigiannis, E. Colacino and I. Halasz, *RSC Mechanochem.* 2025, **2**, 482-487.

31 Q.-L. Shao, Z.-J. Jiang, W.-K Su, *Tetrahedron Lett.* 2018, **59**, 2277–2280. DOI: 10.1016/j.tetlet.2018.04.078.

32 Q. Cao, W. I. Nicholson, A. C. Jones, D. L. Browne, *Org. Biomol. Chem*. 2019, **17**, 1722–1726. DOI: 10.1039/C8OB01781F.

33 K. Kubota, T. Seo, K. Koide, Y. Hasegawa, H. Ito, *Nat. Commun.* 2019, **10**, 111. DOI: 10.1038/s41467-018-08017-9.

34 Q. Lemesre, T. Wiesner, R. Wiechert, E. Rodrigo, S. Triebel, H. Geneste, *Green Chem*. 2022, **24**, 5502–5507. DOI: 10.1039/D2GC01460B.

35 L. A. Panther, D. P. Guest, A. McGown, H. Emerit, R. K. Tareque, A. Jose, C. M. Dadswell, S. J. Coles, G. J. Tizzard, R. González-Méndez, C. A. I. Goodall, M. C. Bagley, J. Spencer, B. W. Greenland, *Chem. Eur. J.* 2022, **28**, e202201444. https://doi.org/10.1002/chem.202201444

36 M. M. Heravi, Z. Kheilkordi, V. Zadsirjan, M. Heydari, M. Malmir, *J. Organomet. Chem.* 2018, **861**, 17–104. DOI: 10.1016/j.jorganchem.2018.02.023.

37 M. A. Topchiy, P. B. Dzhevakov, M. S. Rubina, O. S. Morozov, A. F. Asachenko, M. S. Nechaev, *Eur. J. Org. Chem*. 2016, **2016**, 1908–1914. DOI: 10.1002/ejoc.201501616.

38 J.-S. Ouyang, X. Zhang, B. Pan, H. Zou, A. S. C. Chan, L. Qiu, *Org. Lett*. 2023, **25**, 7491–7496. DOI: 10.1021/acs.orglett.3c02651.

39 P. A. Forero-Cortés, A. M. Haydl, *Org. Process Res. Dev.* 2019, **23**, 1478–1483. DOI: 10.1021/acs.oprd.9b00161.
40 K. Kubota, T. Endo, M. Uesugi, Y. Hayashi, H. Ito, *ChemSusChem* 2022, **15**, e202102132. DOI: 10.1002/cssc.202102132.
41 For reviews and selected examples on liquid-assisted grinding, see: a) L. E. Wenger, T. P. Hanusa, *Chem. Commun.* 2023, **59**, 14210–14222. DOI: 10.1039/D3CC04929A; b) P.Ying, J. Yu and W. Su, *Adv. Synth. Catal.* 2021, **363**, 1246-1271; b) M. Banerjee, A. A. Bhosle, A. Chatterjee and S. Saha, *J. Org. Chem.* 2021, **86**, 13911-13923; c) N. K. Narayanan and M. Schnürch, *ChemCatChem* 2025, **17**, e202401613; d) R. S. Atapalkar and A. A. Kulkarni, *React. Chem. Eng.* 2024, **9**, 10-25; e) L. Chen, M. Regan and J. Mack, *ACS Catal.* 2016, **6**, 868-872; f) M. Arhangelskis, D.-K. Bučar, S. Bordignon, M. R. Chierotti, S. A. Stratford, D. Voinovich, W. Jones and D. Hasa, *Chem. Sci.* 2021, **12**, 3264-3269; g) J. Breinsperger, N. Podlesnik, F. Mele and M. Schnürch, *Chem. Eur. J.* 2026, https://doi.org/10.1002/chem.202503536; h) I. D'Abbrunzo and D. Hasa, *CrystEngComm*, 2026, DOI:10.1039/d5ce00778j; i) H. Luo, Z. Huang, Y. Lai, Y. Jiang, T. Wang and K. Yan, *RSC Mechanochem.* 2026, DOI: 10.1039/d5mr00104h; j) P. Freisa, L. Lattuada, A. Barge and G. Cravotto, *RSC Mechanochem.* 2026, DOI: 10.1039/d5mr00097a; k) J. Templ and L. Borchardt, *Angew. Chem. Int. Ed.* 2026, https://doi.org/10.1002/anie.202523191; l) J. Yu, H. Chen, Z. Zhang, Y. Fang, T. Ying and W. Su, *Green Chem.* 2024, **26**, 6570-6577; m) P. Ying, T. Ying, H. Chen, K. Xiang, W. Su, H. Xie, J. Yu, *Org. Chem. Front.* 2024, **11**, 127-134
42 T. Friščić, S. L. Childs, S. A. A. Rizvi, W. Jones, *CrystEngComm* 2009, **11**, 418–426. DOI: 10.1039/B815174A.
43 K. Kubota, M. Takahashi, F. Puccetti, H. Ito, *Org. Lett.* **2025**, **27**, 22, 5691–5696. DOI: 10.1021/acs.orglett.5c01456.
44 J. L. Howard, Y. Sagatov, L. Repusseau, C. Schotten, D. L. Browne, *Green Chem.* 2017, **19**, 2798–2802. DOI: 10.1039/C6GC03139K.
45 A. Stolle, "Technical Implications of Organic Syntheses in Ball Mills", in Ball Milling Towards Green Synthesis: Applications, Projects, Challenges, Eds.: A. Stolle, B. Ranu, *Royal Society of Chemistry*, Cambridge, 2015, pp. 241-276.
46 S. Lukin, K. Užarević, I. Halasz, *Nat. Protoc.* 2021, **16**, 3492-3521. DOI: 10.1038/s41596-021-00545-x.
47 T. Borchers, F. Topić, M. Arhangelskis, M. Ferguson, C. B. Lennox, P. A. Julien, T. Friščić, *Chem* 2025, **11**, https://doi.org/10.1016/j.chempr.2024.09.018.
48 K. L. Nguyen, T. Friščić, G. M. Day, L. F. Gladden, W. Jones, *Nat. Mater.* 2007, **6**, 206-209. DOI: 10.1038/nmat1848.
49 H. Watanabe, R. Hiraoka, M. Senna, *Tetrahedron Lett*. 2006, **47**, 4481–4484. DOI: 10.1016/j.tetlet.2006.04.030.
50 M. Senna, A. A. L. Michalchuk, *RSC Mechanochem*. 2025. DOI: 10.1039/D4MR00084F.
51 G. Rothenberg, A. P. Downie, C. L. Raston, J. L. Scott, *J. Am. Chem. Soc.* 2001, **123**, 8701-8708. DOI: 10.1021/ja0034388.
52 O. Dolotko, J. W. Wiench, K. W. Dennis, V. K. Pecharsky, V. P. Balempa, *New J. Chem.* 2010, **34**, 25-28. DOI: 10.1039/B9NJ00588A.
53 P. A. Julien, I. Malvestiti, T. Friščić, *Beilstein J. Org. Chem.* 2017, **13**, 2160–2168. DOI: 10.3762/bjoc.13.216.
54 G. Walker, P. Römann, B. Poller, K. Löbmann, H. Grohganz, J.S. Rooney, G. S. Huff, G. P. S. Smith, T. Rades, K. C. Gordon, C. J. Strachan, S. J. Fraser-Miller, *Mol. Pharm.* 2017, **14**, 4675-4684. DOI: 10.1021/acs.molpharmaceut.7b00803.
55 T. Achibat, A. Boukenter, E. Duval, G. Lorentz, S. and Etienne, *J. Chem. Phys.* 1991, **95**, 2949-2954.
56 L. Takacs, *Prog. Mater. Sci.* 2002, **47**, 355-414. DOI: 10.1016/S0079-6425(01)00002-0.
57 a) F. Stoessel, Thermal Safety of Chemical Processes, Risk Assessment and Process Design, 2nd Edition, Wiley-VCH Verlag, Weinheim, Germany (2020).
58 Possibility of inorganic MSR under intense mixing conditions was recently described, see: M. Baláž, P. Jacko, M. Bereš, K. Kenges, L. Mussapyrova, S. S. Shahgoli, M. Podobová, K. Szmuc, G. Gruzel, J. Tulková, I. O. Tampubulon, Y. Shpotyuk, U. Aydemir and T. Stolar, *ChemRxiv*, 2026; doi:10.26434/chemrxiv-2025-l4n3s-v2.
59 B. P. Fors, D. A. Watson, M. R. Biscoe, S. L. Buchwald, *J. Am. Chem. Soc.* 2008, **130**, 13552–13554. DOI: 10.1021/ja8055358.
60 C. Leroy, S. Mittelette, G. Félix, N. Fabregue, J. Špačková, P. Gaveau, T.-X. Métro, D. Laurencin, *Chem. Sci.* 2022, **13**, 6328-6334.
61 G. Zgrablić, A. Senkić, N. Vidović, K. Užarević, D. Čapeta, I. Brekalo, M. Rakić, *Phys. Chem. Chem. Phys.* 2025, **27**, 5909-5920.
62 M. Baláž, R. Džunda, R. Bureš, T. Sopčák, T. Csanádi, *RSC Mechanochem.* 2024, **1**, 94-105.
63 I. Priestley, C. Battilocchio, A. V. Iosub, F. Barreteau, G. W. Bluck, K. B. Ling, K. Ingram, M. Ciaccia, J. A. Leitch, D. L. Browne, *Org. Process Res. Dev*. 2023, **27**, 269–275. DOI: 10.1021/acs.oprd.2c00226.

DATA AVAILABILITY STATEMENT

View Article Online
DOI: 10.1039/D6GC00784H

Details of experimental procedures, along with characterization data, as well as NMR and THz-Raman spectra, thermal monitoring plots and X-ray crystallography information, in PDF format. Also included are crystallographic data in CIF format, which can also be obtained on request free of charge from the Cambridge Crystallographic Data Centre (CCDC), deposition numbers 2372358 and 2372359. The authors have cited additional references within the Supporting Information.[64-67]